Biocatalysis and Agricultural Biotechnology 17 (2019) 7–14

Contents lists available at ScienceDirect

Biocatalysis and Agricultural Biotechnology

journal homepage: www.elsevier.com/locate/bab

Kinetic profiles of the stereoselective reduction of acetophenone and its derivatives promoted by *Galactomyces candidus* GZ1. A mechanistic interpretation

María F. Decarlini[a], Daniela L. Bordón[b], Ana M. Vázquez[a], Gabriela I. Demmel[a], Laura I. Rossi[c], Mario L. Aimar[b,*]

[a] *Laboratorio de Tecnología Química, Facultad de Ciencias Químicas, Universidad Católica de Córdoba, Córdoba, Argentina*
[b] *Cátedra de Química Aplicada, Departamento de Química, Facultad de Ciencias Exactas, Físicas y Naturales, Universidad Nacional de Córdoba, Vélez Sarsfield 1611, Ciudad Universitaria, X5016GCA Córdoba, Argentina*
[c] *Departamento de Química Orgánica, Facultad de Ciencias Químicas, Universidad Nacional de Córdoba, Instituto de Investigaciones en Fisicoquímica de Córdoba (INFIQC) – CONICET, Ciudad Universitaria, X5016GCA Córdoba, Argentina*

ARTICLE INFO

Keywords:
Biocatalysis
1-Phenylethanol
Galactomyces candidus
Stereoinversion
Deracemization

ABSTRACT

A mechanistic interpretation of the kinetic profiles obtained for the stereoselective reduction of acetophenone promoted by *Galactomyces candidus* GZ1 under aerobic and anaerobic conditions was made. Based on experimental and bibliographical data, a mechanism which may involve the participation of two alcohol dehydrogenases with opposite stereoselectivities and alcohol oxidase is discussed. Due to the stereoselectivity of the reduction of acetophenone being changed when anaerobic conditions were used, this microorganism also permitted (*S*)-1-phenylethanol to be obtained in the absence of oxygen. Moreover, the kinetic profiles of the reactions of a racemic mixture of (*R*,*S*)-1-phenylethanol and pure (*S*)-1-phenylethanol with *Gal. candidus* were analyzed, which corroborated that there existed a reaction step where (*S*)-1-phenylethanol was oxidized to acetophenone. The results presented here show that not only is it possible to resolve racemic mixtures of phenylethanols when *Gal. candidus* is used as a biocatalyst, but that this is also efficient in causing the complete stereoinversion of pure (*S*)-1-phenylethanol to (*R*)-1-phenylethanol.

1. Introduction

In recent years, enantiomerically pure alcohols have been mostly produced by the use of biocatalytic systems, since these methodologies are better than general chemical methods in terms of enantioselectivity (Breuer et al., 2004). In this sense, the microbial reduction of prochiral ketones has been widely used for the synthesis of these important chiral synthons (Matsuda et al., 2000). In fact, secondary alcohols are important building blocks for the synthesis of a variety of natural compounds and pharmaceutically relevant products including some marketed drugs (Inoue et al., 2005; Ishikawa et al., 2006; Tanner et al., 1997; Wijdeven et al., 2010).

Biochemical synthetic processes are involved in obtaining these building blocks, which have some comparative advantages over classical chemical procedures, including their low cost, high versatility and efficiency, in addition to highly desirable chemical aspects such as chemo-, regio-, and stereoselectivity (Bennamame et al., 2014, 2015; Huisman et al., 2010; Nakamura and Matsuda, 2006). However, microbial reduction does not afford an alcohol of a satisfactory optical purity when several enzymes of different stereoselectivities are present inside the metabolic system of the microorganism employed as a biocatalyst (Matsuda et al., 2000).

We recently reported the stereoselective reduction of acetophenones and its derivatives using a strain of *Galactomyces candidus* isolated from a decaying carrot (Decarlini et al., 2017). The performance of the reduction system was shown to be extremely efficient (> 99.9 e.e.%) for some substituted acetophenones, and the substrate specificity of the system was also very good. However, it was not clarified at the time how the high stereoselectivity was achieved in addition to important questions such as the required concentration of the substrate, the identity of the co-solvent, and how the relative position of the substituent on the aromatic ring affects the enantiopreference of the product obtained. Therefore, in order to rationalize some of the intrinsic characteristics of the process by which the stereoselective reduction of

---

[*] Correspondence author.
E-mail address: mlaimar@unc.edu.ar (M.L. Aimar).

https://doi.org/10.1016/j.bcab.2018.10.010
Received 7 June 2018; Received in revised form 24 August 2018; Accepted 12 October 2018
Available online 24 October 2018

acetophenone occurs when *Gal. candidus* GZ1 is used as a biocatalyst, a series of experiments were carried out to determine the kinetic profiles of this transformation. In this investigation, a mechanistic interpretation of the kinetic reaction profiles was made, which permits a better understanding of the behavior of *Gal. candidus* GZ1 when used a the biocatalyst in the stereoselective production of 1-phenylethanols. Moreover, the results described in the present work indicate other possible uses of *Gal. candidus* as a biocatalyst in the stereoselective production of chiral alcohols.

2. Materials and methods

2.1. General

Acetophenone (AP) and $NaBH_4$ were purchased from Sigma-Aldrich S.A. (Argentina), and (*S*)-1-phenylethanol ((*S*)-1-PE) and (*R*)-1-phenylethanol ((*R*)-1-PE) were synthesized using methodologies reported in the literature (Aimar et al., 2014; Decarlini et al., 2017). (*R*,*S*)-1-(4'-fluorophenyl)ethanol ((*R*,*S*)-4'F-PE), (*R*,*S*)-1-(4'-chlorophenyl)ethanol ((*R*,*S*)-4'Cl-PE), (*R*,*S*)-1-(4'-bromophenyl)ethanol ((*R*,*S*)-4'Br-PE), (*R*,*S*)-1-(3'-nitrophenyl)ethanol ((*R*,*S*)-3'NO_2-PE), (*R*,*S*)-1-(4'-nitrophenyl) ethanol ((*R*,*S*)-4'NO_2-PE), and (*R*,*S*)-1-(4'-cyanophenyl)ethanol ((*R*,*S*)-4'CN-PE) were synthesized by reduction of the corresponding substituted acetophenones (Aldrich Chemical S.A., Argentina) using $NaBH_4$ in refluxing ethanol. Sterile deionized water was used to prepare the phosphate buffer, and ethyl acetate was purified prior to use. Gas chromatography (GC) analyses were carried out on a Buck Scientific Model 910/310 instrument equipped with a flame ionization detector (FID). GC-mass spectrometry (MS) analyses of the samples were carried out on a Hewlett Packard HP 5890 Series II gas chromatograph equipped with the Mass Detector HP 5970.

2.2. GC-FID and GC-MS analyses

To establish the chromatographic conditions, AP was reduced with $NaBH_4$ in ethanol to obtain a racemic mixture of the 1-phenylethanols with very good yields. The GC separations were carried out on a fused silica capillary column Supelco β-Dex 120 (phenyl polysiloxane with 20% of permethylated β-cyclodextrin, 30 m, 0.25 mm, 0.25 µm) with GC general conditions of split, 145 mL/min; injector, 220 °C; detector FID, 220 °C; carrier gas, N_2; and head pressure, 29 psi, and with the conversion percentages of the reactions being determined by using normalized peak areas without a correction factor. GC conditions: $T_1 = 80\,^{\circ}C$ (1 min), $\Delta T = 2.5\,^{\circ}C/min$, $T_2 = 140\,^{\circ}C$. Retention times of AP, (*S*)-1-PE and (*R*)-1-PE were 14.28, 19.77, and 20.41 min, respectively. The identities of the peaks of the enantiomers in the chromatogram were established using pure (*S*)-1-PE and (*R*)-1-PE as reference standards (Aimar et al., 2014; Decarlini et al., 2017). In addition, the elution order and retention times of the GC data were compared with those reported in the literature for the same column (Orden et al., 2009). The GC-MS (70 eV) analyses were performed using the same conditions as those in the GC analysis, but utilizing a Hewlett Packard HP-5 (Crosslinked 5% PhMeSiloxane, 30 m, 0.32 mm, 0.25 µm film thickness) capillary column.

2.3. Calculation methods for determinations by GC

The conversion ratios of the reactions and their corresponding enantiomeric excesses were determined using the normalized areas of the peaks without a correction factor. To calculate the conversion percentage, Eq. (1) was used:

$$\%\text{conversión} = \frac{A_R + A_S}{A_R + A_S + A_{AP}} \text{ x } 100 \tag{1}$$

The calculation of the enantiomeric excesses was made using Eq. (2):

$$e.\,e.\% = \frac{A_S - A_R}{A_R + A_S} \text{ x } 100 \tag{2}$$

where A_R = Area of the *R*-enantiomer, A_S = Area of the *S*-enantiomer and A_{AP} = Area of acetophenone respectively.

2.4. Kinetic profiles of the stereoselective reduction of AP promoted by Gal. candidus GZ1

The bioreduction methodology used is an adaptation of one described by Ou et al. (2008). *Gal. candidus* GZ1 was grown for 3 days at 25 °C in glucose-peptone-yeast (GPY) broth, and the cells of GZ1 were harvested by filtration. The biomass obtained (≈ 3 g) was suspended in 80 mL of 100 mM sterile solution of phosphate buffer pH 7.0 in a sterile Erlenmeyer of 250 mL, after which, acetophenone (50 µL) dissolved in 1 mL of dimethyl sulfoxide (DMSO) was added. The biotransformation process was developed on an orbital shaker maintained at 150 rpm inside a 25 °C culture oven, with samples (2 mL) being taken at regular time intervals, which were extracted by shaking with ethyl acetate (2 mL). Later, the organic layer was separated, and anhydrous calcium chloride was added to remove the dissolved water. The solution thus obtained was filtered and an aliquot (1 µL) was analyzed by chiral GC-FID and GC-MS. The reaction was carried out in triplicate and the values reported in the figures are the means of these measurements.

2.5. Kinetic profiles of the resolution process of a racemic mixture of (R,S)-1-PE promoted by Gal. candidus GZ1

The methodology used was the same as that described in previous section, but a racemic mixture of (*R*,*S*)-1-PE (50 mg) previously obtained through the reduction of AP with $NaBH_4$ in ethanol was used as the substrate. The reaction was carried out in triplicate, and the values shown in the figures are the means of these measurements.

2.6. Kinetic profiles of the stereoinversion process of (S)-1-PE promoted by Gal. candidus GZ1

The methodology used was the same as that described in previous section, but (*S*)-1-PE (50 mg) previously obtained through the reduction of acetophenone biocatalyzed by fruits of *Ligustrum lucidum* (Aimar et al., 2014) was used as the substrate. The reaction was carried out in triplicate and the values shown in the figures are the mean of these measurements.

2.7. Dynamic kinetic resolution of racemic mixtures of substituted (R,S)-1-PEs promoted by Gal. candidus GZ1

The methodology used was the same as that described in the previous section, but the racemic mixtures of substituted (*R*,*S*)-1-PE (50 mg) described in Table 1 were used as substrates. The valuation and identification of the obtained products was carried out as described by Decarlini et al. (2017).

3. Results and discussion

3.1. Kinetic profiles of the AP reduction reaction promoted by Gal. candidus GZ1

In order to elucidate the process by which *Gal. candidus* GZ1 transforms AP into (*R*)-1-PE, a kinetic study of the reaction was carried out over a period of 32 h, with samples being taken at regular time intervals during the corresponding reactions, and analyzed by chiral GC-FID, as described in experimental section. The results are displayed in Fig. 1.

As can be observed in Fig. 1A, the AP (▲) concentration percentage decreased to 64% (representing approximately a 36% conversion to the

Table 1
Dynamic kinetic resolution of substituted (*R*,*S*)-1-pEs promoted by *Gal. candidus* GZ1.

Entry	R	Time (hs)	Conversion %[a]	e.e.%[a,b]
1	phenyl	48	99[c]	> 99.9(*R*)[c]
2	4'-fluorophenyl	8	69	86 (*R*)
3	4'-chlorophenyl	48	87	> 99.9 (*R*)
4	4'-bromophenyl	48	94	98 (*R*)
5	3'-nitrophenyl	48	60	> 99 (*R*)
6	4'-nitrophenyl	48	88	71 (*R*)
7	4'-cyanophenyl	48	98	> 99.9 (*R*)

[a] Conversion (%) and enantiomeric excess (e.e.%) were determined by chiral GC-FID.
[b] Identification and absolute configurations were assigned according to Decarlini et al. (2017).
[c] Preparative scale reaction.

products) after 5–7 h of reaction. From this moment, the percentage of AP began to increase again until reaching a maximum of 73% (27% conversion) approximately 10 h from the start of the reaction, before falling again until it reached practically zero concentration (24 h of reaction). The appearance of the products was directly related to the variation in the percentage of AP. As can be seen in Fig. 1A, (*S*)-1-PE (■) formed more rapidly than (*R*)-1-PE (♦), with 19% of (*S*)-1-PE being formed during the first hour of reaction, while only 1% of (*R*)-1-PE was observed at this time. The maximum concentration for (*S*)-1-PE was reached approximately after 4–5 h of reaction, and from this point onwards its conversion percentage began to decrease and reached zero approximately 15 h after starting the reaction. It should be noted that when (*S*)-1-PE reached the conversion percentage maximum, this situation coincided with the beginning of the increase in the percentage of AP observed in the reaction medium, which may indicate that *S*-enantiomer was oxidized and gave rise to the formation of AP. In parallel, this percentage of (*R*)-1-PE formation continued to increase over time, but at varying speeds. At 11 h of reaction (where there was a marked decrease in the percentage of (*S*)-1-PE), the system seemed to accelerate towards the accumulation of (*R*)-1-PE, which coincided with the beginning of a second decrease in the percentage of AP. In fact, as can be observed from the first 15 h of reaction, the formation of (*R*)-1-PE was essentially due to a reduction in AP, with the formation percentage of (*R*)-1-PE reaching a maximum, at approximately 24 h of reaction, when both AP and (*S*)-1-PE had disappeared completely.

This interconversion of the enantiomers is shown in Fig. 1B, where the change in the percentage of enantiomeric excess (●) as a function of time is plotted. As can be observed, during the course of the reaction there was a marked variation in the percentage of enantiomeric excess. The reaction began with the formation of the *S*-enantiomer which, little by little, was transformed into the *R*-enantiomer, apparently via previous oxidation to AP (Fig. 1A). Moreover, as can be seen in Fig. 1B, this interconversion process formed a racemic mixture after approximately 8–9 h of reaction, which coincided with an increase in the AP percentage (Fig. 1A). From this moment on, the accumulation of (*R*)-1-PE as a product of the reaction began to predominate.

If (*S*)-1-PE were oxidized to AP and then converted to (*R*)-1-PE, this process may be oxygen dependent. For this reason, and to try to corroborate our observations that there exists a process of oxidation of the *S*-enantiomer, a series of experiments were carried out under anaerobic conditions in an N_2 atmosphere, with the results shown below in Fig. 2.

Fig. 2A shows both the variation of the percentage of the AP concentration and the percentage of the enantiomers appearing over a 10 h reaction period. As can be observed, the absence of O_2 in the reaction medium had a marked effect on the process of reduction of AP (▲) catalyzed by GZ1, with the formation of (*S*)-1-PE (■) being predominant in anaerobic conditions, and reaching an accumulation percentage of approximately 84% after 6 h of reaction. This situation reveals, to our understanding, that there exists an oxidation process from the *S*-enantiomer to AP, with this process being oxygen dependent. Additionally, there was also a small formation of the *R*-enantiomer ((♦) approximately 4%) that began to be evident at 6 h of reaction, possibly formed through the direct and stereoselective reduction of AP. In contrast, as can be observed in the previous figure, AP was consumed

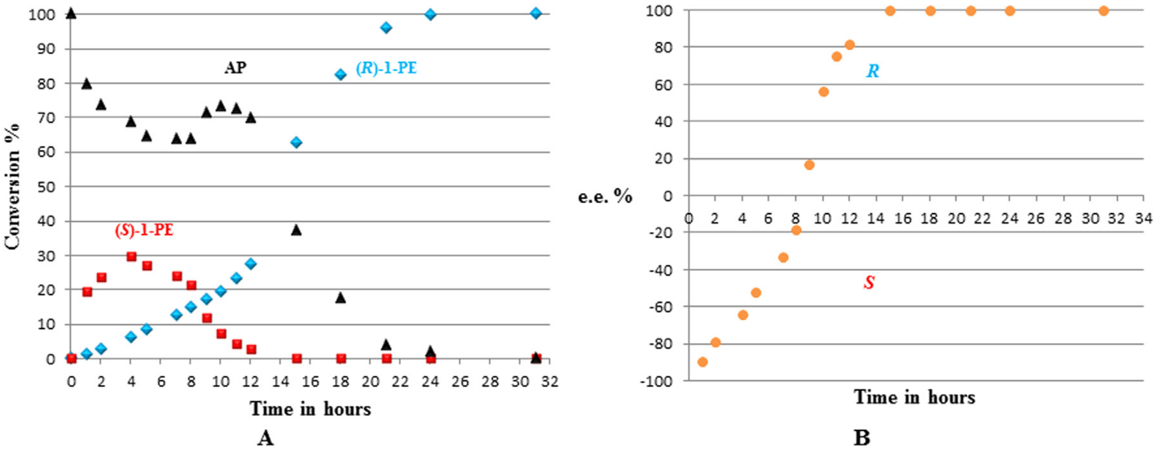

Fig. 1. AP = ▲, (*R*)-1-PE = ♦, (*S*)-1-PE = ■, e.e.% = ●. A) Evolution of the reduction reaction of AP to (*R*)-1-PE catalyzed by *Gal. candidus* GZ1 under aerobic conditions. B) Variation of e.e.% *vs.* time.

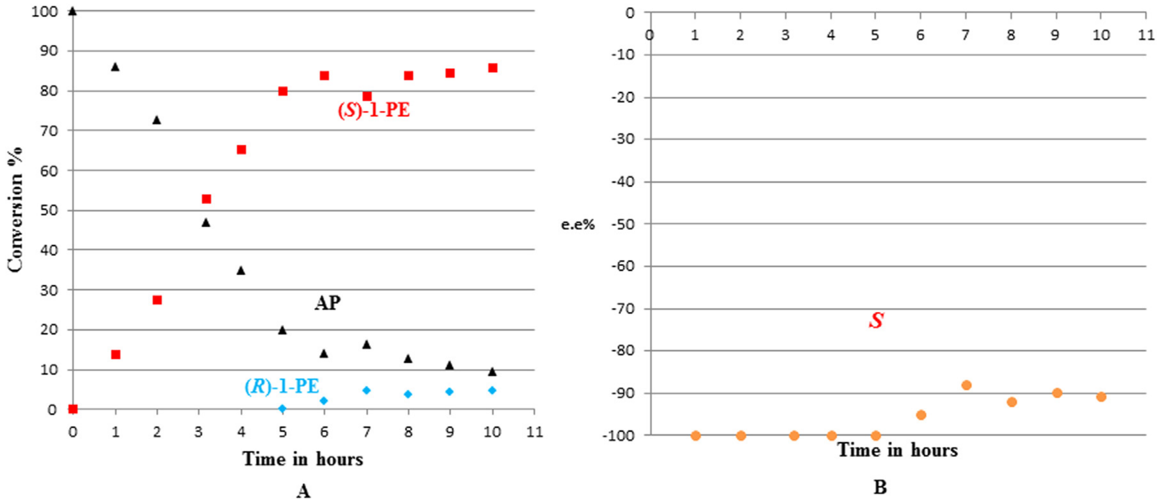

Fig. 2. AP = ▲; (R)-1-PE = ◆; (S)-1-PE = ■; e.e.% = ●. A) Evolution of the reduction reaction of AP catalyzed by *Gal. candidus* GZ1 under anaerobic conditions. B) Variation of e.e.% vs. time.

much more quickly than in the reaction carried out in the presence of oxygen, with the decrease in concentration reaching approximately 90%.

The variation of the enantiomeric excess (●) of the reaction performed under anaerobic conditions is shown in Fig. 2B. It can be observed in this figure that the percentage of enantiomeric excess remained constant (●; > 99.9%) during the first five hours of reaction when the reduction was completely stereoselective for the formation of (S)-1-PE. After this time, the percentage of enantiomeric excess began to change slightly due to the appearance of a very small proportion, of (R)-1-PE (from > 99.9% to ≈ 90 e.e%). From here onwards, the e.e.% remained approximately constant.

Based on the observations made during the course of our experiments under both aerobic (Fig. 1) and anaerobic conditions (Fig. 2), it is possible to postulate a stereoselective reduction mechanism of AP promoted by *Gal. candidus* GZ1, as shown in Fig. 3.

As can be observed in Fig. 3, the AP reduction process may be made up of two well-differentiated steps: a phase of an apparently irreversible reduction of AP to promote the formation of (R)-1-PE, and a reversible reduction - oxidation stage that promoted the formation of (S)-1-PE, where the oxidation stage was oxygen dependent. The reduction of AP was established quickly (first 6 h, Fig. 1A), with the formation of (S)-1-PE, which, little by little, changed towards the formation of (R)-1-PE through an apparently irreversible reduction process. The mechanism proposed in Fig. 3 can justify the data shown in Fig. 1A if the relationship between the values of the velocity constants is of the form $k_3 \geq k_2 > > k_1$. This assumption also coincides (Fig. 1A) with the fact that the formation of (S)-1-PE and its subsequent disappearance occurred more rapidly than the conversion of AP to (R)-1-PE. Additionally, the change in rate observed for the reaction after 10 h (Fig. 1A), where a modification (acceleration) is seen in the slope of the function that describes the formation of (R)-1-PE, also coincides with this speculative relationship of the rate constants.

This fact shows, to our understanding, that within the metabolic system of *Gal. candidus* GZ1, two alcohol dehydrogenases (ADHs) with opposite stereoselectivities can coexist, with one ADH providing the formation of (R)-1-PE in a form apparently irreversible, and another catalyzing the formation of (S)-1-PE. In agreement with our interpretations, it should be noted that systems of this type have already been described and postulated for other microorganisms, such as *Candida parapsilosis* ATCC 7330 (Baskar et al., 2005; Kaliaperumal et al., 2011; Nie et al., 2011), *Candida albicans* CCT 0776 (Mantovani et al., 2009), *Cunninghamella echinulata* NRRL 1384 (Cardus et al., 2004), *Nocardia fusca* AKU 2123 (Xie et al., 1999), and *Geotrichum candidum* IFO 5767 (Nakamura et al., 1995 and 2001), among others. Related to this, Grüber et al. (2006) described a system, with the involvement of a consecutive reduction-oxidation reaction system for this type of transformations. The net redox balance of this process is zero (in an ideal case) with no external cofactor recycling being necessary, since the redox equivalents, such as NAD(P)H, are being recycled internally between two steps. Furthermore, it was proposed that molecular oxygen might be involved in cofactor regeneration, because stereoinversion was faster under aerobic conditions (Azerad and Buisson, 1992; Kometani et al., 1996; Nakamura et al., 2001), suggesting the involvement of an alcohol oxidase rather than a reversible alcohol dehydrogenase. Additionally, our reaction system involves the use of DMSO and this cosolvent produced a marked improvement in the percentage of conversion as was opportunely reported by our work team (Decarlini et al., 2017). This situation, perhaps, could be indicating the participation of the DMSO in the recycling of the cofactors in the same path proposed for other substances such as ethanol, which was occasionally supplied as a co-solvent to increase the solubility of the substrate (Chadha and Baskar, 2002; Grüber et al., 2006). However, more studies are necessary to support this hypothesis.

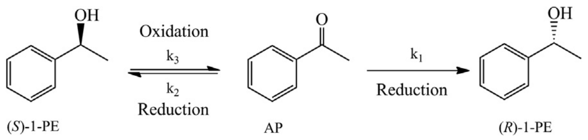

Fig. 3. Proposed mechanism for the reduction of AP promoted by *Gal. candidus* GZ1.

In addition to the kinetic studies of the reductive process, we also tried to the inhibit both ADHs in separate experiments in order to force the reaction to go through one of the paths proposed in the mechanism described in Fig. 3, specifically by attempting to inhibit the steps described by k_1 and by k_2. It has been described in the literature (Padhi and Chadha, 2005; Padhi et al., 2004) that there are different chemical substances capable of producing the selective inhibition of these enzymes, and therefore when ADHs coexist with opposite stereoselectivities, it is possible to select the path that the transformation will travel. Therefore, separate experiments using allyl alcohol (Dahl et al., 1999) and allyl bromide (Dahl et al., 1999; Davoli et al., 1999; Nakamura et al., 2003) as possible inhibitors were carried out at different concentrations, but the results achieved were not satisfactory and the stereoselectivity of the reaction was not changed. In this case, only a marked inhibition of the total reductive process was observed.

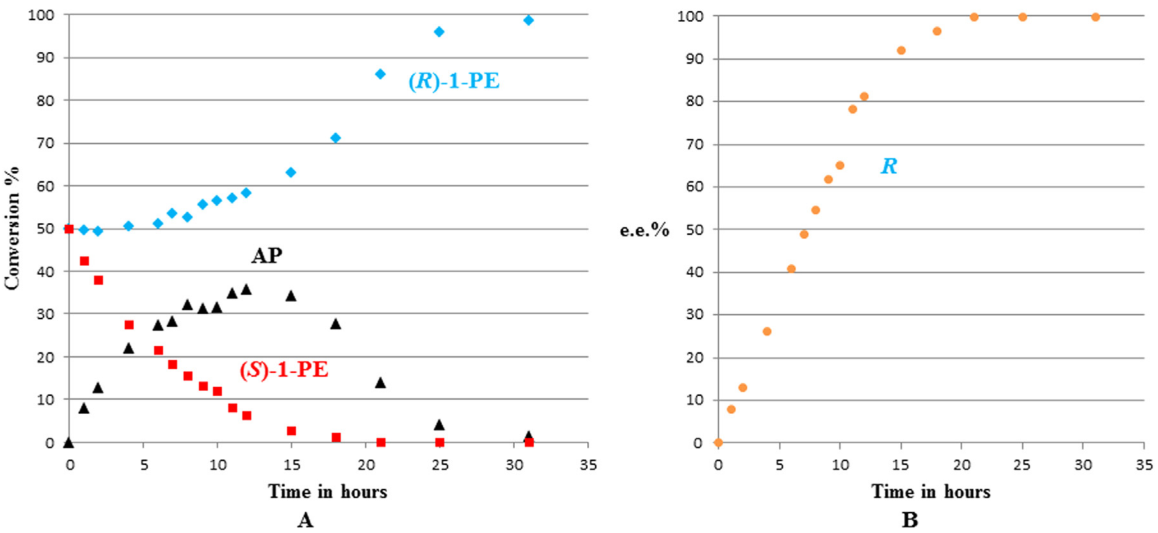

Fig. 4. AP = ▲; (*R*)-1-PE = ♦; (*S*)-1-PE = ■; e.e.% = ●. A) Kinetics profile of the dynamic kinetic resolution of a racemic mixture of (*R*, S)-1-PEs promoted by *Gal. candidus* GZ1 under aerobic conditions. B) Variation of e.e.% vs. time.

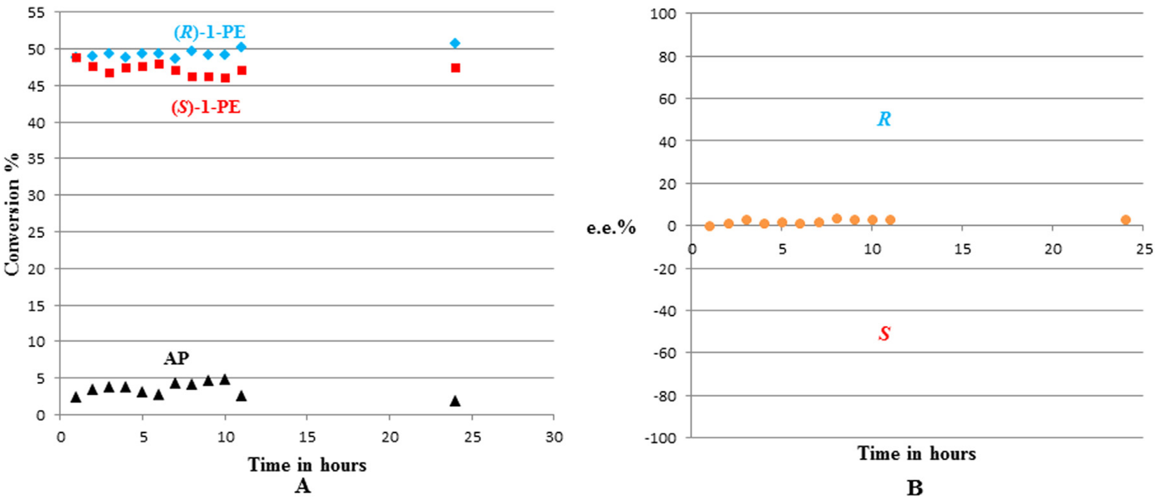

Fig. 5. AP = ▲; (*R*)-1-PE = ♦; (*S*)-1-PE = ■; e.e.% = ●. A) Kinetics profile of the dynamic kinetic resolution of a racemic mixture of (*R*, *S*)-1-PE promoted by *Gal. candidus* GZ1 under anaerobic conditions. B) Variation of e.e.% vs. time.

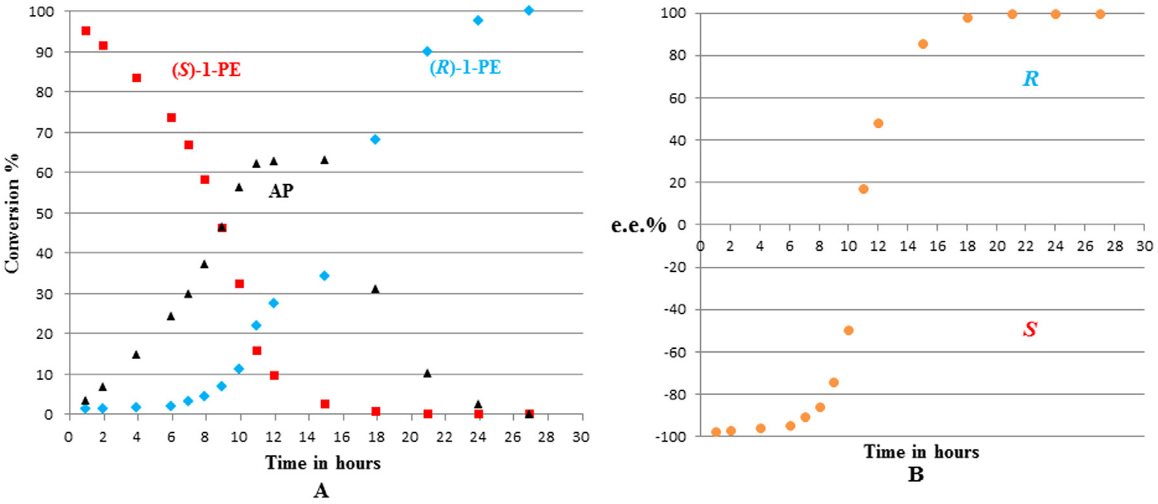

Fig. 6. AP = ▲; (*R*)-1-PE = ♦; (*S*)-1-PE = ■; e.e.% = ●. A) Stereoinversion reaction of pure (*S*)-1-PE promoted by *Gal. candidus* GZ1 under aerobic conditions. B) Variation of e.e.% over time.

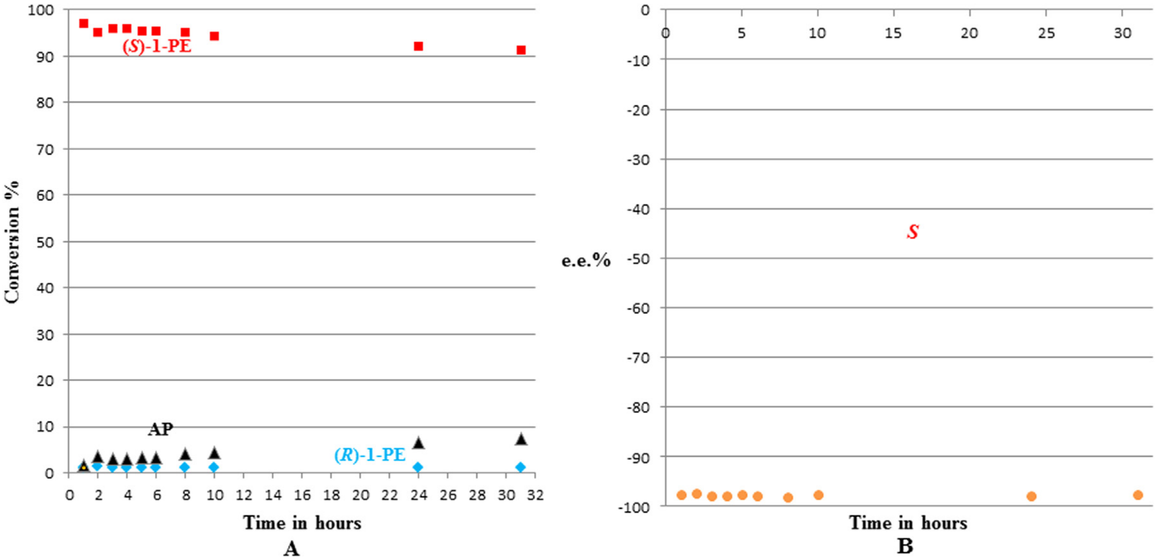

Fig. 7. AP = ▲; (*R*)-1-PE = ♦; (*S*)-1-PE = ■; e.e.% = ●. A) Stereoinversion process of (*S*)-1-PE promoted by *Gal. candidus* GZ1 under anaerobic conditions. B) Variation of e.e.% over time.

3.2. Kinetic profiles of the resolution process of a racemic mixture of (R,S)-1-PE promoted by Gal. candidus GZ1

Considering the results obtained in the previous experiments, it was decided to investigate further the process of bioreduction of AP promoted by *Gal. candidus* GZ1. If our interpretations concerning the data provided by the kinetic profiles shown in Figs. 1 and 2 were correct, then it would be possible to use *Gal. candidus* GZ1 to resolve a racemic mixture of (*R*,*S*)-1-PE and to perform a deracemization by stereoinversion of the *S*-enantiomer. To carry this out, a racemic mixture of (*R*,*S*)-1-PE with GZ1 as the biocatalyst was used, with the results shown in Fig. 4.

This figure shows the variation of the concentration of AP (▲), the disappearance percentage of the enantiomer (*S*)-1-PE (■) and the formation of the enantiomer (*R*)-1-PE (♦) during a period of 32 h of reaction. As can be observed, when the concentration of (*S*)-1-PE began to decrease, AP started to form and its concentration increased, while the concentration of (*R*)-1-PE remained constant until approximately 6 h after starting the reaction. Moreover, on observing the variation in the concentration of both AP and (*S*)-1-FE, it can be seen that the crossing point in the evolution of the concentrations occurred approximately after 5 h of reaction, and at this moment the percentage of variation was 25% for both species. This observation, together with the fact that the concentration percentage of (*R*)-1-PE remained constant during this period of time, clearly shows that the *S*-enantiomer was oxidized to promote AP formation, as postulated in the proposed mechanism shown in Fig. 3. As the reaction proceeded, the concentration of AP continued to increase until it reached a maximum of ≈ 36% (after 12 h of reaction). From here onwards, the concentration of AP began to decrease in parallel with the increase in the concentration of (*R*)-1-PE. The reaction was completed at approximately 25–30 h, where the complete disappearance of AP and (*S*)-1-PE as well as the complete formation of *R*-enantiomer can be observed. Furthermore, at 20 h of reaction, the *S*-enantiomer had practically disappeared, while the AP concentration that still persisted in the reaction medium (≈ 20%) continued to be reduced to form (*R*)-1-PE, in a similar way as observed with the data shown in Fig. 1A. In Fig. 4B, the variation of the enantiomeric excess as a function of time is shown, and this graphic clearly shows how the enantiomeric excess of the reaction mixture changes in favor of the formation of (*R*)-1-PE. Nevertheless, the reaction became completely stereoselective at approximately 20 h, despite still there AP in the reaction medium (Fig. 4A).

Additionally, a resolution reaction of the racemic mixture of (*R*,*S*)-1-PE by *Gal. candidus* GZ1was also carried out under anaerobic conditions, with the results being displayed in Fig. 5.

It can be observed in Fig. 5A, during the resolution of racemic mixture of (*R*,*S*)-1-PEs under anaerobic conditions (absence of O_2), there was only a small decrease in the concentration of (*S*)-1-PE (■), with a parallel appearance of AP (▲), while the concentration of (*R*)-1-PE (♦) remained approximately constant over 24 h. In the same way, Fig. 5B shows that the percentage of enantiomeric excesses remains practically unchanged.

In summary, the results obtained using a racemic mixture consisting of (*R*,*S*)-1-PE clearly support the proposed mechanism described in Fig. 3. Moreover, it is worth emphasizing the importance of the results presented here because the classical resolution of a racemic mixture is based on the difference between physical properties of the diastereoisomers, which previously must be formed and separated by conventional methods, implying that the performance associated with this process cannot be higher than 50% in the best of cases. In contrast, using a resolution process by stereoinversion, such as that reported here, allowed us to obtain one of the enantiomers of the mixture with almost 100% theoretical yield. This situation clearly represents another potential use of *Gal. candidus* GZ1 as a microorganism able to carry out, in an extraordinarily efficient way, the resolution of a racemic mixture of (*R*,*S*)-1-PE by stereoinversion of the *S*-enantiomer to obtain the *anti*-Prelog product.

3.3. Kinetic profiles of the stereoinversion process of (S)-1-PE promoted by Gal. candidus GZ1

In classical chemistry, there are two well-known processes that permit the inversion of the configuration of an alcoholic stereogenic center, namely the classic S_N2 reactions and the Mitsunobu´s reaction (March, 2007). Both methodologies allow the configuration of an alcoholic chiral center to be inverted, but each of these has its limitations. Due to the results obtained in our kinetic studies, we decided to study the possibility of totally inverting the configuration of pure (*S*)-1-PE through its exposure to *Gal. candidus* GZ1, and the results are shown below in Fig. 6.

As can be seen in Fig. 6A, during the first six hours of reaction the percentage of (*S*)-1-PE (■) decreased whereas the AP (▲) concentration increased, corroborating that observed in our previous experiments. However, the formation percentage of (*R*)-1-PE (♦) was minimal over

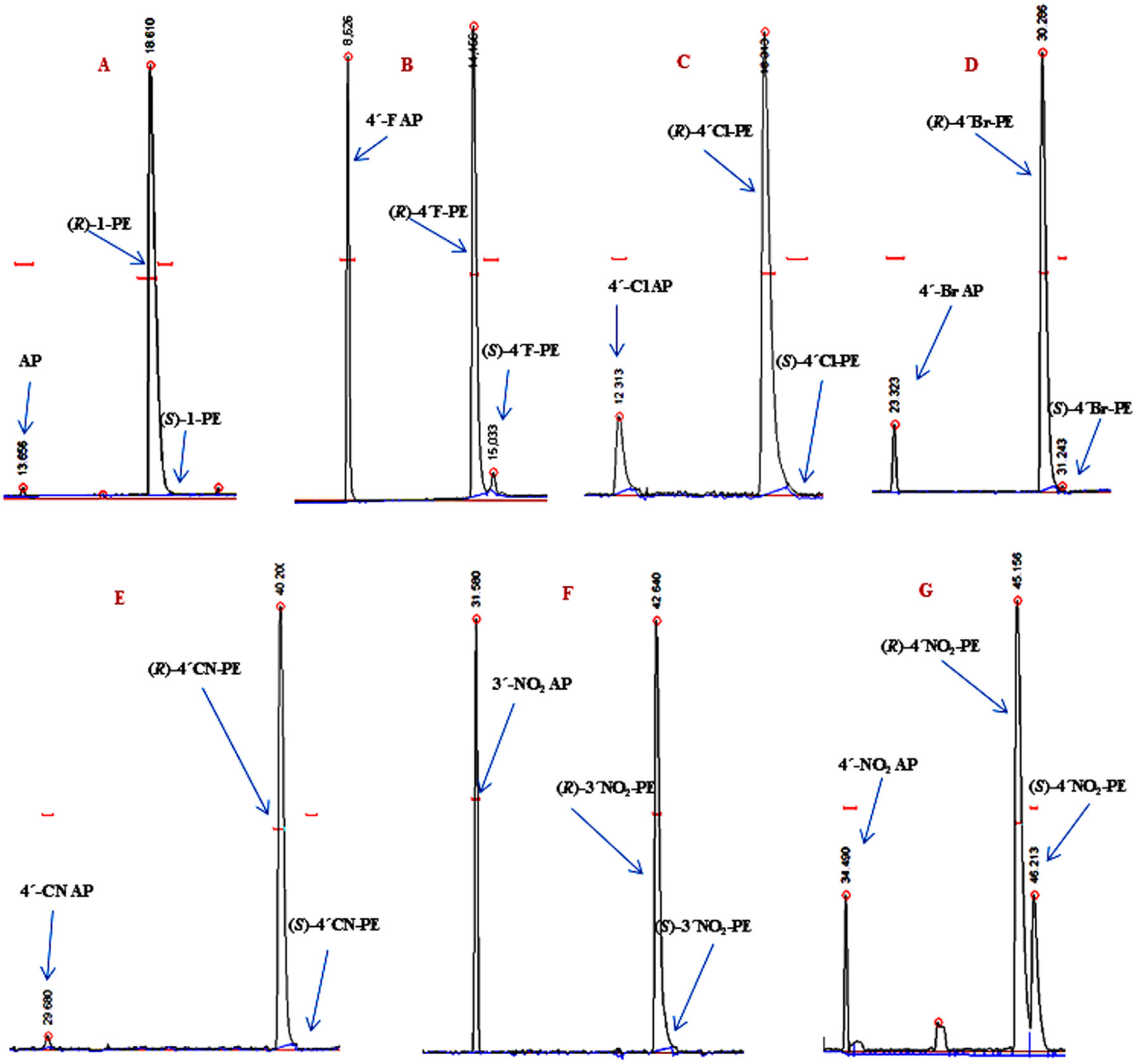

Fig. 8. Final chromatograms of dynamic kinetic resolution of substituted (*R*, *S*)-1-PEs promoted by GZ1. A) (*R*, *S*)-1-(phenyl)ethanol (48 h of reaction), B) (*R*, *S*)-1-(4'-Flurophenyl)ethanol (8 h) C) (*R*, *S*)-1-(4'-Chlorophenyl)ethanol (48 h), D) (*R*, *S*)-1-(4'-Bromophenyl)ethanol (48 h), E) (*R*, *S*)-1-(4'-Cyanophenyl)ethanol (48 h), F) (*R*, *S*)-1-(3'-Nitrophenyl)ethanol (48 h), G) (*R*, *S*)-1-(4'-Nitrophenyl)ethanol (48 h).

the same period of time. Moreover, after 12 h of reaction, the concentration of (*S*)-1-PE had decreased by approximately 90%, and the percentage of the formation of AP reached a maximum that remained almost constant between 10 and 16 h after the beginning of the reaction. During this time period, the formation of (*R*)-1-PE increased markedly from 10% (10 reaction hours) to approximately 70% (16 reaction hours). Finally, the reaction was completed approximately after 24 h, which resulted in the total, efficient and stereoselective conversion of (*S*)-1-PE to (*R*)-1-PE. In Fig. 6B, the variation of the enantiomeric excess is displayed as a function of the time, and here it can be clearly observed that the *S*-enantiomer was completely into the *R*-enantiomer.

As can be observed in this Figure, (*S*)-1-PE was converted stereoselectively to (*R*)-1-PE in approximately 18–20 h of reaction, with the transformation processes involved in the mechanism postulated in Fig. 3 being in agreement with the results of this experiments.

Finally, a stereoinversion reaction was also performed under anaerobic conditions using (*S*)-1-PE and *Gal. candidus* GZ1 as the biocatalyst, and the results are shown in Fig. 7.

As can be seen in Fig. 7A, the performance of the stereoinversion reaction from (*S*)-1-PE (🟥) to (*R*)-1-PE (♦) under anaerobic conditions (atmosphere of N_2) was almost totally inhibited, demonstrating once again that the transformation reaction required the presence of oxygen to fulfill the oxidation process of (*S*)-1-PE to form AP (▲). In addition, the small formation of AP observed during the course of the reaction was directly related to the decrease in the concentration of (*S*)-1-PE and it may have been due to a small amount of oxygen present into the system. Finally, it is important to note that the e.e.% (●) remained almost constant over 32 h of reaction (Fig. 7B).

3.4. Dynamic kinetic resolution of racemic mixtures of substituted (R,S)-1-PEs promoted by Gal. candidus GZ1

As mentioned above, the resolution of racemic samples by stereoinversion of one enantiomer is a very important methodology because a theoretical yield of 100% is possible. The results observed using *Gal. candidus* GZ1 as biocatalyst in the dynamic kinetic resolution of a racemic mixture of (*R*,*S*)-1-PE encouraged us to study the resolution of racemic mixtures of substituted (*R*,*S*)-1-PEs in the same system, as a way to generalize the application of this biological reducer and to reinforce our mechanistic hypothesis about its procedure. These results are shown in Table 1.

It can be seen in Table 1 that *Gal. candidus GZ1* was an efficient biocatalyst for resolving six racemic mixtures of substituted (*R*,*S*)-1-PEs to their corresponding *R*-alcohols, with conversions ranging from 60% to 98%, (Table 1, entries 4 and 6 respectively), and with most of the products having satisfactory optical purities. In this sense, an excellent performance with (*R*,*S*)-4'CN-PE was observed in 48 hs of reaction (Table 1, entry 6). On the other hand, it is interesting to note that the formation and disappearance of the corresponding substituted acetophenone derivatives was observed in all experiments (Fig. 8A-G), and these observations clearly agree with the proposed mechanism shown in Fig. 3.

Additionally, it should be noted that the biocatalyst resolved all racemic samples without observing Prelog's rule. On the other hand, it should be mentioned that the procedure for the resolution of the racemic mixtures reported here was not optimized and the reactions were simply carried out in the conditions used to solve (*R*,*S*)-1-PE.

3.5. *Preparative scale reaction of (R)-1-PE by dynamic kinetic resolution of (R,S)-1-PE using GZ1*

Due to the importance of the results obtained when a racemic sample of (*R*,*S*)-1-PE was resolved with GZ1, a preparative scale reaction was performed. To carry this out, 1.012 g of (*R*,*S*)-1-PE was reacted with 35 g GZ1, 10 mL of DMSO in a final volume of 800 mL of phosphate buffer pH 7,0, at 150 rpm and 25 °C. The reduction was performed in 48 h and (*R*)-1-PE was obtained with 99% of conversion and > 99.9 of e.e.% (Fig. 8A). The extraction of the product was performed with ethyl acetate using a liquid-liquid extractor. The dried residue was purified by column chromatography using hexane / ethyl acetate mixtures in variable portions as the eluent and the isolated yield of the product was 79% (0.804 g). It should be noted that the extraction and purification procedures were not optimized.

4. Conclusions

The results from the kinetic profiles obtained under both aerobic and anaerobic conditions using *Gal. candidus* GZ1 as the biocatalyst show that the metabolic process by which the transformation of AP to (*R*)-1-PE is carried out takes place in three stages. This process could involve at least two ADH enzymes that have opposite stereoselectivities, with one of these having a reversible effect (*S*-ADH) while the other (*R*-ADH) performs the transformation in an apparently irreversible way. Moreover, as the reversibility of the *S*-enantiomer formation is oxygen dependent, this situation raises the possibility of an alcohol oxidase enzyme being involved in the mechanism rather than a reversible *S*-ADH. For this reason, three enzymes may be involved in the transformation process. However, more studies are necessary to support this hypothesis.

The studies presented here show that *Gal. candidus* GZ1 is not only an efficient biological reductant to obtain (*R*)-1-PE in a totally stereoselective way from AP, but also by performing the reaction under anaerobic conditions, it is possible to invert the configuration of the final product, and in this way, to obtain (*S*)-1-PE using the same microorganism.

Finally, it should be noted that the results obtained using the racemic mixtures of substituted (*R*,*S*)-1-PEs and pure (*S*)-1-PE to promote the stereoselective formation of the corresponding *R*-enantiomers reveal two other potential uses of *Gal. candidus* GZ1, which widens its field of application as a biocatalyst. Related to this, further studies are currently being carried out in our laboratory.

Acknowledgments

María F. Decarlini and Ana M. Vazquez gratefully acknowledge financial support from the Universidad Católica de Córdoba, (UCC), Argentina. Mario L. Aimar gratefully acknowledges financial support from Secretaría de Ciencia y Tecnología de la Universidad Nacional de Córdoba, (SECyT-UNC), Argentina (Grant no. 30720150100338CB). Laura I. Rossi is research from CONICET. We thank Dr Paul Hobson, native speaker, for the revision of this manuscript. This work is dedicated in recognition of the teaching career of Dr Elba I. Buján.

References

Aimar, M.L., Bordón, D.L., Formica, S.M., Cantero, J.J., Vazquez, A.M., Velasco, M.I., Rossi, L.I., 2014. Fruits of the glossy privet (Ligustrum lucidum –Oleaceae) as biocatalysts for producing chiral aromatic alcohols. Biocat. Biotrans. 32, 348–357.

Azerad, R., Buisson, D., 1992. Microbial reagents in organic synthesis. In: Servi, S. (Ed.), NATO ASI Series C 381. Kluwer Academic Publishers, Dordrecht Netherlands, pp. 421–440.

Baskar, B., Pandian, N.G., Priya, K., Chadha, A., 2005. Deracemisation of aryl substituted α-hydroxy esters using Candida parapsilosis ATCC 7330: effect of substrate structure and mechanism. Tetrahedron 61, 12296–12306.

Bennamame, M., Zeror, S., Aribi-Zouioueche, L., 2014. Asymmetric reduction of ketones by biocatalysis using medlar (Mespilus germanica **L.**) fruit grown in Algeria. Biocat. Biotrans. 32 (5–6), 327–332.

Bennamame, M., Zeror, S., Aribi-Zouioueche, L., 2015. Asymmetric reduction of ketones by biocatalysis using clementine mandarin (citrus reticulata) fruit grown in Annaba or by ruthenium catalysis for access to both enantiomers. Chirality 27, 205–210.

Breuer, M., Ditrich, K., Habicher, T., Hauer, B., Kebeler, M., Sturmer, R., Zelinski, T., 2004. Industrial methods for the production of optically active intermediates. Angew. Chem. Int. Ed. 43, 788–824.

Cardus, G.J., Carnell, A.J., Trauthweinb, H., Riermeir, T., 2004. Microbial deracemisation of N-(1-hydroxy-1-phenylethyl)benzamide. Tetrahedron: Asymmetry 15, 239–243.

Chadha, A., Baskar, B., 2002. Biocatalytic deracemisation of α-hydroxy esters: high yield preparation of (*S*)-ethyl 2-hydroxy-4-phenylbutanoate from the racemate. Tetrahedron: Asymmetry 13, 1461–1464.

Dahl, A.C., Fjeldberg, M., Madsen, J.O., 1999. Baker's yeast: improving the d-stereoselectivity in reduction of 3-oxo esters. Tetrahedron: Asymmetry 10, 551–559.

Davoli, P., Forni, A., Moretti, I., Prati, F., Torre, G., 1999. (R)-(+) and (S)-(−) ethyl 4,4,4-trifluoro-3-hydroxy butanoate by enantioselective baker's yeast reduction. Enzym. Microb. Tech. 25 (1–2), 149–152.

Decarlini, M.F., Aimar, M.L., Vázquez, A.M., Vero, S., Rossi, L.I., Yang, P., 2017. Fungi isolated from food samples for an efficient stereoselective production of phenylethanols. Biocat. Agric. Biotech. 12, 275–285.

Grüber, C.C., Lavandera, I., Faber, K., Kroutil, W., 2006. From a racemate to a single enantiomer: deracemisation by stereoinversion. Adv. Synth. Catal. 348, 1789–1805.

Huisman, G.W., Liang, J., Krebber, A., 2010. Practical chiral alcohol manufacture using ketoreductases. Curr. Opin. Chem. Biol. 14, 122–129.

Inoue, K., Makino, Y., Itoh, N., 2005. Production of (*R*)-chiral alcohols by a hydrogen-transfer bioreduction with NADH-dependent *Leifsonia* alcohol dehydrogenase (LSADH). Tetrahedron: Asymmetry 16, 2539–2549.

Ishikawa, M., Hiraiwa, Y., Kubota, D., Tsushima, M., Watanabe, T., Murakami, S., Ouchi, S., Ajito, K., 2006. Tricyclic pharmacophore-based molecules as novel integrin $\alpha_v\beta_3$ antagonists. Part III: synthesis of potent antagonists with $\alpha_v\beta_3/\alpha_{IIb}\beta_3$ dual activity and improved water solubility. Bioorg. Med. Chem. 14, 2131–2150.

Kaliaperumal, T., Gummadi, S.N., Chadha, A., 2011. *Candida parapsilosis* ATCC 7330 can also deracemise 1-arylethanols. Biocatal. Biotrans. 29 (6), 262–270.

Kometani, T., Yoshii, H., Matsuno, R., 1996. Large-scale production of chiral alcohols with bakers' yeast. J. Mol. Catal. B: Enzym. 1, 45–52.

Mantovani, S.M., Angolini, C.F.F., Marsaioli, A.J., 2009. Mechanistic investigation of the Candida albicans CCT 0776 stereoinversion system and application to obtain enantiopure secondary alcohols. Tetrahedron: Asymmetry 20, 2635–2638.

Matsuda, T., Harada, T., Nakajima, N., Nakamura, K., 2000. Mechanism for improving stereoselectivity for asymmetric reduction using acetone powder of microorganism. Tetrahedron Lett. 41, 4135–4138.

March, J.T., 2007. In: Smith, M.B., March, J. (Eds.), Advanced Organic Chemistry, Six edition. Wiley-Interscience a John Jiley & Sons, Inc..

Nakamura, K., Fujii, M., Ida, Y., 2001. Stereoinversion of arylethanols by *Geotrichum candidum*. Tetrahedron: Asymmetry 12, 3147–3153.

Nakamura, K., Inoue, Y., Matsuda, T., Ohno, A., 1995. Microbial deracemization of 1-arylethanol. Tetrahedron Lett. 36, 6263–6266.

Nakamura, K., Matsuda, T., 2006. Biocatalytic reduction of carbonyl group. Curr. Org. Chem. 10, 1217–1246.

Nakamura, K., Yamanaka, R., Matsuda, T., Harada, T., 2003. Recent developments in asymmetric reduction of ketones with biocatalysts. Tetrahedron: Asymmetry 14, 2659–2681.

Nie, Y., Xiao, R., Xu, Y., Montelione, G.T., 2011. Novel anti-Prelog stereospecific carbonyl reductases from *Candida parapsilosis* for asymmetric reduction of prochiral ketones. Org. Biomol. Chem. 9, 4070–4078.

Orden, A.A., Magallanes-Noguera, C., Agostini, E., Kurina-Sanz, M., 2009. Anti-Prelog reduction of ketones by hairy root cultures. J. Mol. Catal. B: Enzym. 61, 216–220.

Ou, Z., Wu, J., Yang, L., Cen, P., 2008. Asymmetric reduction of chloroacetophenones to produce chiral alcohols with microorganisms. Korean J. Chem. Eng. 25 (1), 124–128.

Padhi, S.K., Chadha, A., 2005. Deracemisation of aromatic β-hydroxy esters using immobilised whole cells of *Candida parapsilosis* ATCC 7330 and determination of absolute configuration by ^{1}H NMR. Tetrahedron: Asymmetry 16, 2790–2798.

Padhi, S.K., Pandian, N.G., Chadha, A., 2004. Microbial deracemisation of aromatic β-hydroxy acid esters. J. Mol. Catal. B: Enzym 29, 25–29.

Tanner, D., Tedenborg, L., Almario, A., Pettersson, I., Csöregh, I., Kelly, N.M., Andersson, P.G., Högberg, T., 1997. Total synthesis of balanol, part 2. Completion of the synthesis and investigation of the structure and reactivity of two key heterocyclic intermediates. Tetrahedron 53, 4857–4868.

Wijdeven, M.A., Willemsen, J., Rutjes, F.P.J.T., 2010. The 3-hydroxypiperidine skeleton: key element in natural product synthesis. Eur. J. Org. Chem. 15, 2831–2844.

Xie, S.-X., Ogawa, J., Shimizu, S., 1999. Production of (R)-3-pentyn-2-ol through stereoinversion of racemic 3-pentyn-2-ol by Nocardia fusca AKU 2123. Appl. Microbiol. Biotechnol. 52, 327–331.